Doublecortin-like Kinase Controls Neurogenesis by Regulating Mitotic Spindles and M Phase Progression

Tianzhi Shu,[1] Huang-Chun Tseng,[1,2,5] Tamar Sapir,[4,5] Patrick Stern,[3] Ying Zhou,[1,2] Kamon Sanada,[1] Andre Fischer,[1] Frédéric M. Coquelle,[4] Orly Reiner,[4] and Li-Huei Tsai[1,2,*]

[1] Department of Pathology
Harvard Medical School and
[2] Howard Hughes Medical Institute
77 Avenue Louis Pasteur
Boston, Massachusetts 02115
[3] Center for Cancer Research
Massachusetts Institution of Technology
Cambridge, Massachusetts 02139
[4] Department of Molecular Genetics
The Weizmann Institute of Science
76100 Rehovot
Israel

Summary

The mechanisms controlling neurogenesis during brain development remain relatively unknown. Through a differential protein screen with developmental versus mature neural tissues, we identified a group of developmentally enriched microtubule-associated proteins (MAPs) including doublecortin-like kinase (DCLK), a protein that shares high homology with doublecortin (DCX). DCLK, but not DCX, is highly expressed in regions of active neurogenesis in the neocortex and cerebellum. Through a dynein-dependent mechanism, DCLK regulates the formation of bipolar mitotic spindles and the proper transition from prometaphase to metaphase during mitosis. In cultured cortical neural progenitors, DCLK RNAi Lentivirus disrupts the structure of mitotic spindles and the progression of M phase, causing an increase of cell-cycle exit index and an ectopic commitment to a neuronal fate. Furthermore, both DCLK gain and loss of function in vivo specifically promote a neuronal identity in neural progenitors. These data provide evidence that DCLK controls mitotic division by regulating spindle formation and also determines the fate of neural progenitors during cortical neurogenesis.

Introduction

The mammalian brain undergoes pronounced cytoarchitectural changes during development. Through mitotic division, neural progenitor cells give rise to lineages of neurons. These neurons then migrate, often over long distances, to their final positions (Caviness et al., 2003; Gupta et al., 2002). Neuronal proliferation and migration are temporally and spatially coordinated to construct the distinctive structure of the central nervous system. For instance, the neocortex, which exhibits six layers of neurons, is built through precisely orchestrated waves of newly born neurons that migrate past their predecessors (Gupta et al., 2002). After migration, neuronal polarity is established upon the specification of the axon and dendrites (Horton and Ehlers, 2003), which is followed by elaborate axonal targeting, dendritic arborization, and synaptogenesis (Huber et al., 2003; Tessier-Lavigne and Goodman, 1996).

Diverse as they are, these morphological changes are executed through dynamic rearrangement of the cytoskeletal network components, such as microtubules and actin filaments (Baas, 1999; Huber et al., 2003; Tucker, 1990). The microtubule network undergoes drastic changes in neural cells at different developmental stages. For instance, during neural proliferation, microtubules assemble into the highly organized mitotic spindle upon the entry of mitosis (Ohnuma and Harris, 2002). Recent studies suggest that the orientation of the mitotic spindle may determine the mode of neural division (Haydar et al., 2003; Kaltschmidt et al., 2000). After the postmitotic neurons are generated, they extend a directional leading process and migrate toward their destination, the cortical plate. During migration, another specific microtubule network couples the centrosome and nucleus, resulting in the salient translocation of the nucleus (Shu et al., 2004; Solecki et al., 2004; Tanaka et al., 2004a; Xie et al., 2003).

Microtubule-associated proteins (MAPs) have been shown to be the direct regulators of microtubule dynamics during many of these developmental processes (Paglini et al., 2000; Sanchez et al., 2000; Tucker, 1990). Through genetic approaches, two genes responsible for human type I lissencephaly, *LIS1* and *DCX*, were identified (Gleeson et al., 1998; Hattori et al., 1994; Reiner et al., 1993). LIS1 and DCX are both MAPs that regulate microtubule dynamics in vitro and in vivo (Gleeson et al., 1999; Sapir et al., 1997). Depletion of LIS1 or DCX by either a genetic or RNAi approach causes severe neuronal migration and positioning defects in the neocortex (Bai et al., 2003; Cahana et al., 2001; Hirotsune et al., 1998). Other studies further showed that LIS1 forms a complex with NudE-like protein 1 (Ndel1) and dynein, and this complex is implicated in orchestrating nucleokinesis during cortical neuronal migration by sustaining the microtubule network that couples the centrosome and nucleus (Shu et al., 2004; Smith et al., 2000). In migrating cerebellar granule neurons, DCX also consolidates this microtubule network through the interaction with LIS1 and dynein (Tanaka et al., 2004a).

To identify MAPs with novel functions during brain development, we performed a differential protein screen on developmental and mature neural tissues. One of the most intriguing MAPs that we identified in our screen was doublecortin-like kinase (DCLK), a protein that shares 70% homology in the N-terminal domain with DCX. The C-terminal domain of DCLK, however, contains a kinase domain homologous to CaM kinase II (Burgess et al., 1999). The DCLK gene is extremely complex, and it has been reported that at least nine alternative products exist (Burgess and Reiner, 2000, 2002). In this study, we investigated the role of DCLK and provided evidence that

*Correspondence: li-huei_tsai@hms.harvard.edu
[5] These authors contributed equally to this work.

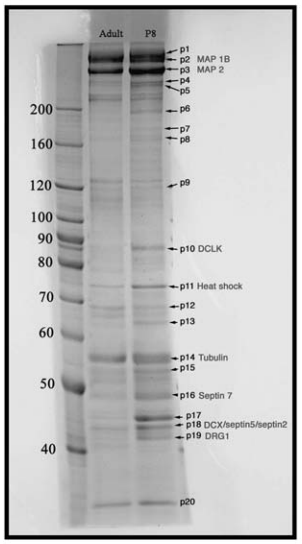

B

Protein band	Score	Molecular weigh (kDa)	A no.	Protein
P1	233	194.2	Q9Z0R4	Mouse Intersectin 1 (EH and SH3 domains protein 1)
	173	188.7	Q9Z0R6	Mouse intersectin 2
P2	2010	270.4	P14873	Mouse MAP 1B (1.2)
	290	188.7	Q9Z0R6	Mouse intersectin 2
	240	191.7	P33173	Mouse KIF1A
P3	1.239e+05	198.9	P20357	Mouse MAP 2
P4	68.4	185	Q62234	Mouse Myomesin 1 (Skelemin)
P5	33.6	140.6	P97820	Mouse mitogen-activated protein kinase kinase kinase kinase 4 (MEKKK4)
P6	256	215.7	Q8R418	Mouse endoribonuclease Dicer
P7	17.1	98	Q61824	Mouse ADAM 12 precursor
P8	45.7	194	O35134	Mouse DNA-directed RNA polymerase I largest subunit
P9	40.3	92.7	Q61056	Mouyse short transient receptor potential channel 1
	39.6	115.8	Q9QVP9	Mouse Focal adhesion kinase 2
P10	**6.264e+04**	**84.1**	**Q9JLM8**	**Mouse DCLK**
P11	9.992e+04	70.8	P08109	Mouse heat shock cognate 71 kDa protein
P12				unidentified
P13	334	49.5	Q62288	Mouse Testican-1 precursor
P14	1.367e+04	50.1	P02551	Mouse tubulin alpha-1
	4958	50.4	Q9ERD7	Mouse tubulin beta-3
P15	636	77.8	Q9Z0Z0	Mouse cGMP-dependent protein kinase 1, beta isozyme
P16	264	50.5	Q9WVC0	Rat septin 7 (CDC 10 homolog)
	263	50.5	O55131	Mouse septin 7 (CDC 10 homolog)
P17	901	79.5	Q61847	Mouse meprin A beta-subunit precursor
P18	5181	40.6	O88809	Mouse Doublecortin
	822	40.2	Q9Z2Q6	Mouse Septin 5
	228	41.5	P42208	Mouse Septin 2 (Nedd 5)
P19	1118	40.5	P32233	Mouse developmentally regulated GTP-binding protein 1 (DRG1; Nedd 3)
P20	1243	63.6	Q9R1C6	Diacylglycerol kinase

C

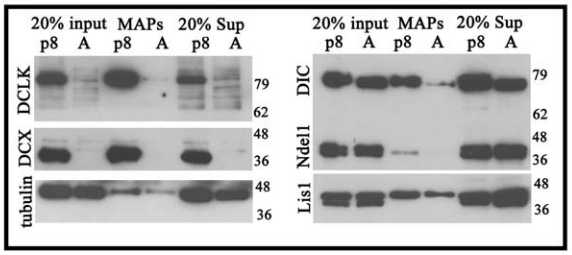

Figure 1. Identification of MAPs Enriched during Neural Development

(A) MAPs were purified from P8 and adult cerebellum, respectively, and resolved on a protein gel. After Coomassie blue staining, the protein bands that show differential pattern between the two ages (indicated by arrows and named p1–p20) were dissected out for MALD-TOF MS.

(B) Results of the protein identification. Note that protein band p10 was identified as mouse DCLK.

(C) Western blot confirmed that identified MAPs such as DCLK and DCX are enriched during development, and a large portion of these proteins is found associated with microtubules (compared to the amount in the supernatant). It should be noted that other MAPs such as the Ndel1/LIS1/dynein complex does not show similar enrichment in developing neural tissues and a smaller proportion of these proteins is found associated with microtubules.

DCLK regulates the structure and dynamics of the mitotic spindles and further controls neural division and fate determination during cortical development.

Results

Doublecortin-like Kinase Is a Microtubule-Associated Protein Enriched during Development

To identify microtubule-associated proteins (MAPs) with potentially novel functions during neural development, we performed a protein-based differential screen. MAPs were purified from postnatal day (P) 8 and adult (>8 weeks) cerebellum by a standard biochemical method (see Experimental Procedures). Cerebellum was chosen as the tissue source for MAPs purification because it undergoes dramatic morphological changes during early postnatal stages including active neurogenesis, neuronal migration, and differentiation (Goldowitz and Hamre, 1998). In addition, the cerebellum provides sufficient tissue mass for the large-scale protein purification. MAPs were purified from P8 and adult cerebellar lysates. Purified MAPs were resolved on a SDS-PAGE gel and counter-stained with Coomassie blue. Many protein bands were found to be preferentially present in MAPs from P8 cerebellum (indicated by arrows in Figure1A). These protein bands were dissected out and digested with trypsin for peptide fingerprint identification by MALDI-TOF mass spectrometry. Among the identified proteins, two homologous proteins, doublecortin (DCX) and doublecortin-like kinase (DCLK) were found among the MAPs enriched on P8 (Figures 1A and 1B). DCLK was originally identified as KIAA0369 through a homologous comparison with DCX on its N terminus (Burgess et al., 1999). Like DCX, DCLK is able to polymerize microtubules in vitro, suggesting a role in regulating microtubule dynamics (Burgess and Reiner, 2000; Lin et al., 2000). The function of DCLK during neural development, however, remains largely unknown.

Western blots were performed with specific antibodies against DCLK and DCX to confirm the results of the differential screen. Both DCLK and DCX were found predominantly expressed in P8 cerebellum compared to adult. A significant portion of DCLK (about 50%) and DCX (about 25%) was associated with microtubules, suggesting an active shuffling of these proteins between a microtubule associated form and a cytosolic form (Figure 1C). This differential expression profile was specific to DCLK and DCX because none of Ndel1, LIS1, and dynein displayed a similar pattern (Figure 1C). The observation that DCX and DCLK are more highly associated with microtubules compared to motor-based MAPs suggests that DCX and DCLK may exert different but more robust functions in regulating microtubules during development.

DCLK Is Expressed in the Neural Progenitor Cells

Immunostaining with an antibody generated against the C-terminal of DCLK showed that similar to DCX, DCLK was highly expressed in P8 cerebellum, including the external granule layer (EGL) (arrowheads in Figure 2A) and the internal granule layer (IGL) (arrows in Figure 2A). By contrast, the expression of DCLK and DCX were nearly

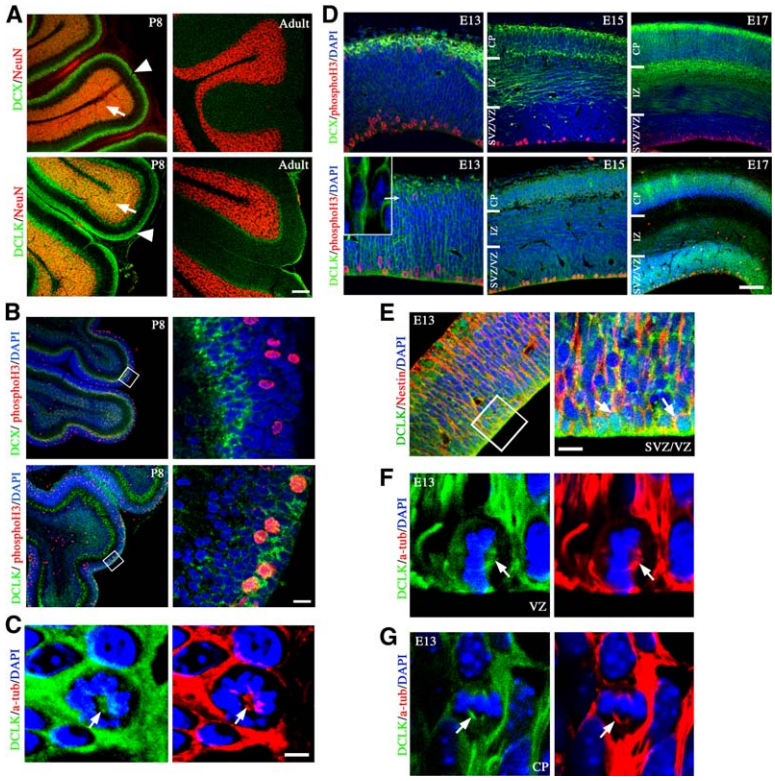

Figure 2. Expression of DCLK in Brain Regions of Neurogenesis

(A) In cerebellum, both DCX and DCLK are highly expressed in the external granule layer (EGL, arrowheads) and internal granule layer (IGL, arrows) on P8, and their expression is drastically diminished in adult.

(B) Coimmunostaining with phophoH3 shows that DCLK is highly expressed in the outer zone of EGL and DCX is expressed in the inner zone of EGL (the high-power panels indicate the boxed region).

(C) DCLK is expressed in the mitotic spindle in a cerebellar neural progenitor at prometaphase.

(D) The expression of DCX and DCLK during cortical development. The staining of phophoH3 indicates dividing neural progenitors. The inset shows the migrating neurons in the cortex indicated by the arrow.

(E) On E13, DCLK is expressed in radial glia lining the ventricle wall (arrowheads). The high-power panel shows the boxed region.

(F and G) The expression of DCLK associated with mitotic spindle in dividing progenitors lining the ventricle wall (F) or located within the CP (G). Scale bar in (A) = 80 μm in P8 cerebellum and 50 μm in adult cerebellum; bar in (B) = 100 μm in lower power and 10 μm in higher power. Bar in (C) = 2.5 μm, also in (F) and (G); bar in (D) = 60 μm in E13 panel, 80 μm in E15 panel, and 100 μm in E17 panel; bar in (E) = 60 μm in the low-power panel and 15 μm in the high-power panel.

absent in the adult cerebellum (Figure 2A). Although DCX was expressed in the inner zone of the EGL, DCLK was largely restricted to the outer zone, where dividing neural progenitors labeled with mitotic marker phosph-H3 were located (Figure 2B, the boxed areas were shown in high power). Immunolabeling of the postmitotic neurons with NeuN further showed an overlap with DCX in the inner zone of EGL (data not shown). Closer inspection of EGL progenitors with confocal z series further revealed that DCLK was expressed in the mitotic spindle (arrows in Figure 2C indicate a cell at prometaphase).

In the developing neocortex, DCLK was also expressed in the active region of neurogenesis, the subventricular and ventricular zones (SVZ/VZ) (Figure 2D). Consistent with previous studies (Burgess and Reiner, 2002; Gleeson et al., 1999; Lin et al., 2000), we found that throughout development (from E13 to E17), DCX expression was largely excluded from the SVZ/VZ in which phosphoH3-positive neural progenitors were located (Figure 2D). On E13, DCLK was found expressed in the marginal zone, cortical plate (CP), and the SVZ/VZ (Figure 2D; inset shows the migrating neurons in the CP). DCLK was expressed in radial glia labeled with an antibody against nestin (arrowheads in Figure 2E point to two cell bodies in the VZ). In dividing neural progenitors lining the surface of the ventricular wall, the expression of DCLK was associated with the mitotic spindle (arrows in Figure 2F point to a cell at metaphase). Similar observation is also made in dividing neural progenitors located in other regions such as the CP (Figure 2G shows a metaphase cell in the CP). On E15 and E17, expression of DCLK was high in the CP and the SVZ/VZ and relatively lower in the intermediate zone (IZ) (Figure 2D).

We also examined the expression pattern of DCX and DCLK in cultured neural progenitors, which were isolated from E14 mouse cortices and maintained in a defined medium containing bFGF-2. Double immunostaining with Nestin showed that DCLK, but not DCX, was expressed throughout the cytoplasm in the neural progenitors (Figure S1). In cultured dividing neural progenitors, the expression of DCLK was also found associated closely with mitotic spindles (Figure S1).

DCLK Induces Monopolar Mitotic Spindles and Arrests Mitosis at Prometaphase

To directly test whether DCLK regulates the formation of mitotic spindles, we overexpressed EGFP-tagged wild-type DCLK in 293 HEK cells as a mean of gain of function. At interphase, DCLK gain of function dramatically induced microtubule polymerization, which formed pronounced ring-like structures (arrowhead in Figure 3A). Interestingly, at M phase, DCLK induced large monopolar mitotic spindles. These abnormal spindles usually extended several thick and rigid branches (arrow in Figure 3A), displaying striking differences from the stereotypical bipolar spindles in cells transfected with EGFP alone (Figure S2). Analysis of the mitotic index (the percentage of mitotic cells) showed no significant difference between control and DCLK gain of function, suggesting that the balance of M phase entry and exit was not disrupted (Figure 3B). However, an obvious abnormality was observed regarding the distribution of the mitotic cells overexpressing DCLK. Although control cells were distributed across all mitotic phases, including prometaphase, metaphase, anaphase, and telophase, cells with DCLK gain of function were mostly arrested at

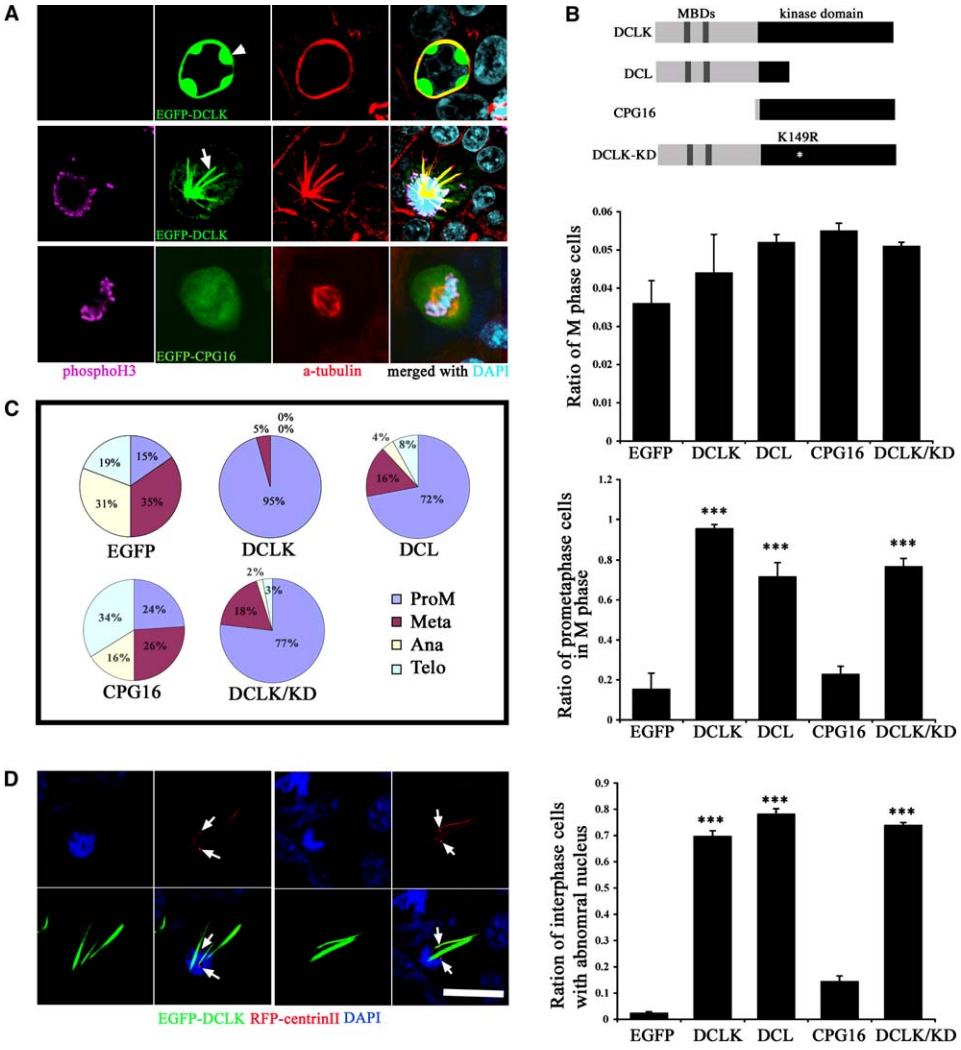

Figure 3. DCLK Gain of Function Induces Monopolar Mitotic Spindles and Arrests Mitotic Cells at Prometaphase

(A) Overexpression of DCLK-EGFP construct in HEK293 cells induces microtubule bundling. At interphase, the hyperpolymerized microtubules are evident by both EGFP (green) and α-tubulin staining (red). At M phase, overexpression of DCLK-EGFP induces a large monopolar spindle that extends thick and stiff branches. Overexpression of CPG-16 fails to induce such monopolar spindle at M phase.

(B) Schematic of splice variants of DCLK and quantification of the effects on mitotic index, M phase arrest, and nuclear morphology after the overexpression of DCLK, DCL, CPG16, and DCLK kinase-dead form (total number of the analyzed cells are 721, 502, 926, 1370, and 684 for control, DCLK, DCL, CPG16, and DCLK-KD, respectively). Number of the mitotic cells are 26, 22, 48, 75, and 35, respectively.

(C) Pie graph of effect of DCLK gain of function on the distribution of mitotic cells in different phases.

(D) Centrosome is labeled with RFP-CentrinII in cells arrested at prometaphase after DCLK gain of function. The centrosome displays normal morphology (arrows in [D] point to centrosome). Scale bar in (D) = 10 μm in (A) and 25 μm in (D). Repeated student t tests between control and different experimental groups were performed, and triple asterisk indicates $p < 0.001$.

prometaphase (95% compared to 15% in control) (Figures 3B and 3C). In addition, we observed frequent occurrences of nuclear abnormalities such as meganuclei, double nuclei, and fragmented nuclei at interphase of cells overexpressing DCLK, which was likely the consequence of the M phase arrest (Figure 3C and data not shown).

Next, we investigated which domain of DCLK was responsible for inducing the abnormal mitotic spindles and M phase arrest. Two natural splice variants of DCLK, the N terminus splicing form, doublecortin like (DCL; GenBank accession AF155821) and the C-terminal form, Candidate Plasticity Gene 16 (CPG16; GenBank accession AF155820) were used in these experiments (Burgess and Reiner, 2002). DCL contains the tandem microtubule binding domain (MBD) but not the kinase domain while CPG16 contains almost exclusively the kinase domain (Figure 3B). In addition, a previously reported DCLK kinase-dead form (K149R) was also included to test whether the kinase activity was required (Lin et al., 2000). Similar to DCLK, overexpression of either DCL or DCLK kinase dead induced large monopolar mitotic spindle and caused a comparable arrest of M phase progression (72% and 77% of M phase cells were arrested at prometaphase, respectively) (Figures 3B and 3C). CPG16, however, exerted no effect on either the mitotic spindles or M phase progression (Figure 3A–3C). These experiments showed that the N terminus of DCLK with the tandem MTB domains is necessary and sufficient to disrupt normal spindle formation and to cause M phase

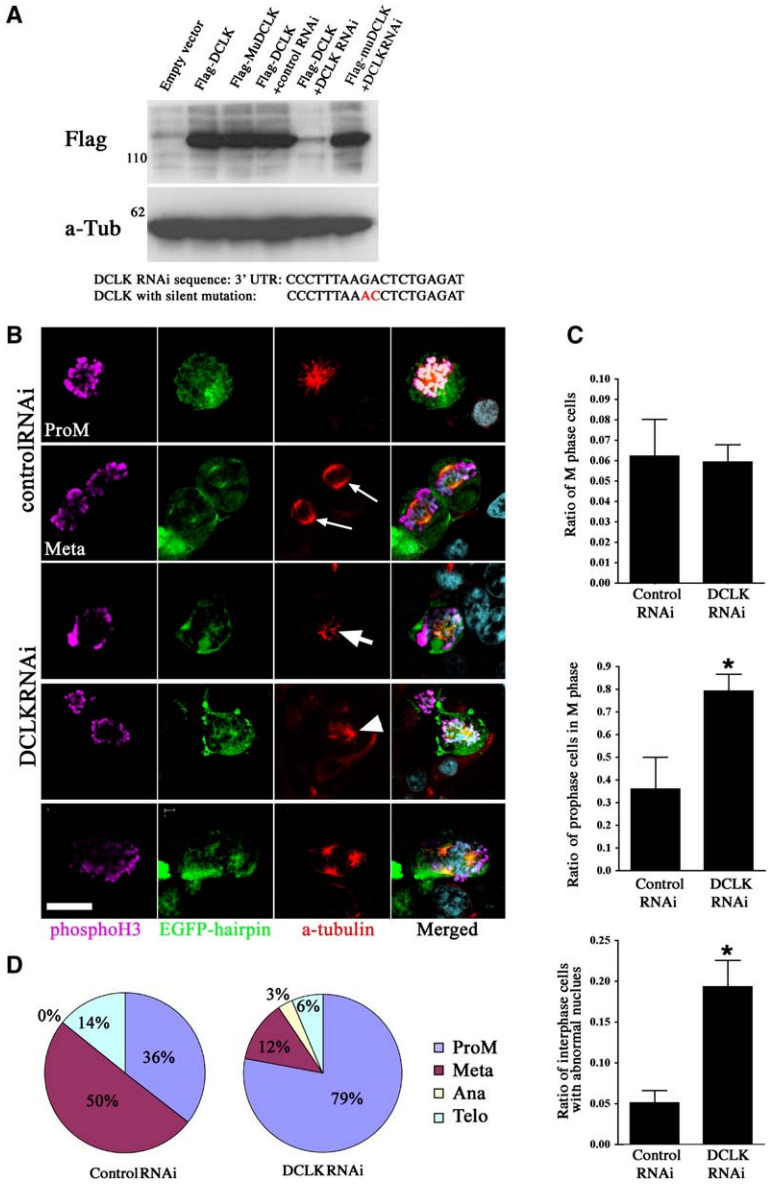

Figure 4. DCLK Loss of Function Disrupts Spindle Formation and Causes Prometaphase Arrest

(A) DCLK RNAi or control RNAi vector was transfected in HEK293 cells to silence the forced expression of FLAG-DCLK wild-type or FLAG-DCLK with two silent mutations (red letters).

(B) 293 cells were transfected with control or DCLK RNAi. Control RNAi has no effect on the progression of M phase or the formation of mitotic spindles. Many metaphase cells could be seen with typical bipolar spindles (thin arrows). Cells transfected with DCLK RNAi were mostly arrested at prometaphase. Formation of the mitotic spindles in these cells is disrupted. Significantly shorter (thick arrow) and abnormal asymmetrical spindles (arrowhead) are predominant. Multipolar spindles were also seen.

(C) Quantification of the effect of DCLK RNAi on mitotic index, M phase arrest, and nuclear morphology. Pie graph of effect of DCLK loss of function on the distribution of mitotic cells in different phases. A significant percentage of cells treated with DCLK RNAi were arrested at prometaphase. Scale bar in (B) = 10 μm. Student t test was performed, and asterisk indicates $p < 0.01$.

arrest, whereas the kinase domain and/or the kinase activity are dispensable.

To examine whether the formation of monopolar spindles is due to centrosomal abnormalities, we labeled the centrosome with RFP-centrinII. The centrosome in the interphase cells appeared normal when DCLK was overexpressed (Figure S3). At M phase, even though cells were arrested at prometaphase, two well-separated centrosomes were readily detected (arrows in Figure 3D), suggesting that the formation of monopolar spindles was not due to a centrosomal defect. Interestingly, the monopolar spindles induced by DCLK did not appear to originate from the centrosome, suggesting that DCLK is potentially capable of inducing mitotic spindle assembly independent of the centrosome (Figure 3D).

DCLK Loss of Function Disrupts Mitotic Spindles and M Phase Progression

To examine the effect of DCLK loss of function, we developed an RNA interference (RNAi) construct targeting the 3′UTR region of DCLK. This RNAi construct significantly reduced the expression levels of wild-type DCLK (Figure 4A). The specificity of the RNAi was further demonstrated by using a DCLK cDNA with two silent mutations within the targeted sequence. The forced expression of this mutant DCLK was not silenced by the RNAi construct (Figure 4A).

Transfection of HEK293 cells with control RNAi did not affect the morphology of mitotic spindles (thin arrows in Figure 4B point to bipolar spindles at metaphase). In addition, the M phase progression was normal as mitotic cells proceeded through metaphase to telophase (Figures 4B–4D). By contrast, DCLK RNAi treatment induced an obvious disorganization of the mitotic spindles. In most cases, the mitotic spindles appeared significantly smaller because the spindle pole emanated much shorter and thinner microtubule branches (thick arrow in Figure 4B). At prometaphase, asymmetrical spindles with branches extending toward one pole were predominant (arrowhead in Figure 4B). Multiple spindles

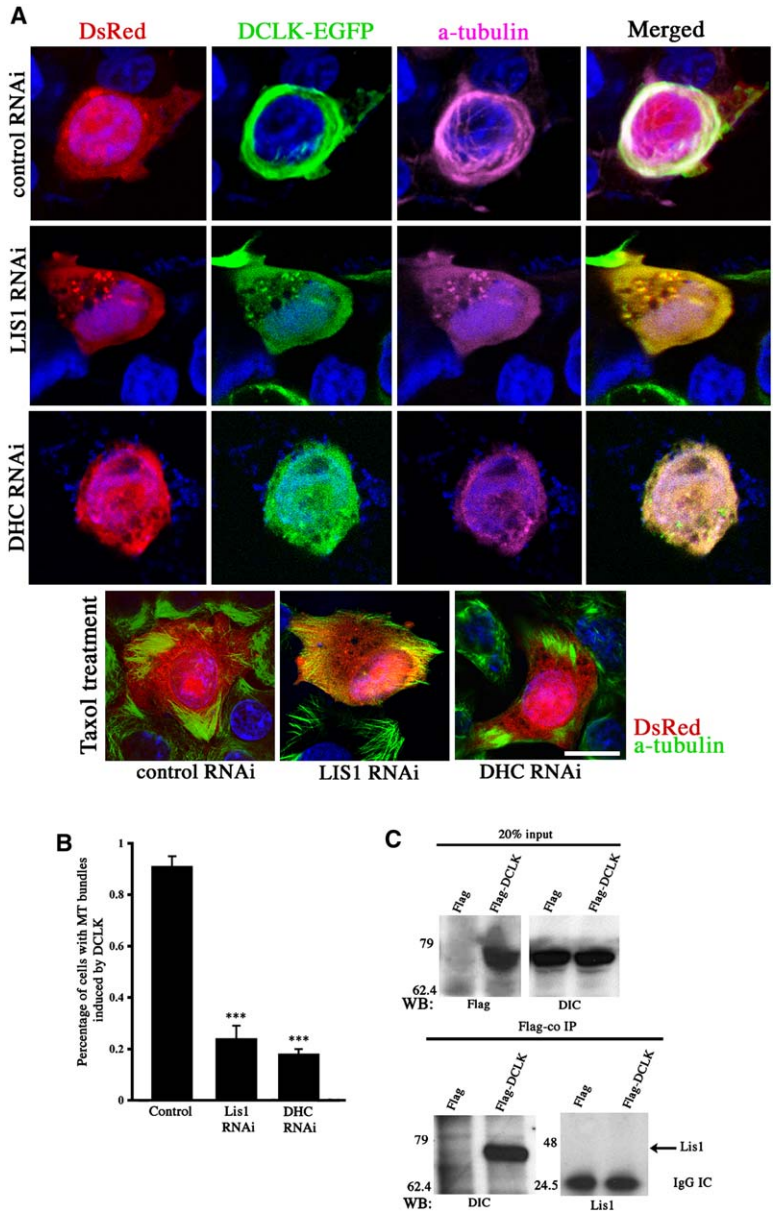

Figure 5. The Function of DCLK to Assemble Microtubules Is Dynein Dependent

(A) HEK293 cells were treated with control RNAi vector or RNAi vectors against LIS1 and dynein heavy chain (DHC) with DsRed construct for 48 hr followed by the transfection of DCLK-GFAP vector for 24 hr. DCLK induces microtubule polymerization in cells treated with control RNAi but not with LIS1 or DHC RNAi. Taxol treatment (50 nM for 2 hr) induces microtubule polymerization in all conditions.

(B) Quantification of the percentage of cells with microtubule bundles induced by DCLK-EGFP.

(C) Coimmunoprecipitation with a FLAG antibody pulls down dynein intermediate chain (DIC) from cells lysate with overexpression of FLAG-DCLK. Scale bar in (A) = 10 μm. Student t test was performed, and triple askterisk indicates $p < 0.001$.

were also frequently observed (bottom in Figure 4B). As M phase progressed, these abnormal spindles did not separate or migrate to the two poles, and the bipolar spindles failed to form. Consequently, 79% of the mitotic cells were arrested at prometaphase (Figures 4C and 4D). In addition, a significant percentage of cells also displayed a wide range of nuclear abnormalities similar to those observed in DCLK gain-of-function experiments (Figure 4C and data not shown).

The Function of DCLK to Assemble Microtubule Is Dynein Dependent

As a microtubule-based motor, dynein complex has been shown to play important roles in microtubule network assembly and dynamics in both mitotic and postmitotic cells (Rusan et al., 2002; Shu et al., 2004; Tanaka et al., 2004a). To test whether the function of DCLK to assemble microtubules is dependent on dynein activity, we inhibited dynein activity by using RNAi against dynein heavy chain (DHC) or Lis1, a positive regulator of dynein motor (Smith et al., 2000; Shu et al., 2004). HEK293 cells were transfected with control, DHC, or LIS1 RNAi in conjunction with DsRed vector at a ration of 10:1. After 48 to 72 hr, cells were transfected with DCLK-EGFP vector. Cells were fixed 24 hr later for α-tubulin staining. In cells transfected with control RNAi, DCLK induced pronounced microtubule polymerization (Figure 5A). However, in a significant percentage of cells treated with DHC or LIS1 RNAi, DCLK failed to assemble microtubules (Figure 5A). Taxol, a compound that induces microtubule polymerization, is still capable of inducing microtubule assembly in cells treated with DHC or LIS1 RNAi, suggesting that the tubulin monomers in cells treated with LIS1 or DHC RNAi have the potential to polymerize; however, the function of DCLK to induce such polymerization is dependent upon Lis1 and dynein activity.

To seek evidence of a physical interaction between DCLK and dynein, we performed coimmunoprecipitation experiments. HEK293 cells were transfected with either FLAG-DCLK or control FLAG vector. Immunoprecipitation with FLAG antibody pulled down dynein intermediate chain (DIC) from cell lysates transfected with FLAG-DCLK but not control FLAG vector (Figure 5C). However, no significant amount of LIS1 was coimmunopreciptated with DCLK (Figure 5C). This result suggests that the function of DCLK to assemble microtubules may depend on its direct interaction with the dynein motor complex, which may play a role in shuttling DCLK from the cytosol to the microtubules.

DCLK Controls the Mitotic Division and Fate Determination of Cultured Neural Progenitors

We next examined whether DCLK controls spindle formation and mitotic progression during proliferation of neural progenitors. To sufficiently silence DCLK gene expression in neural progenitors, we generated a DCLK RNAi lentiviral vector. DCLK RNAi hairpin sequence was subcloned into a lentiviral vector under the control of U6 promoter. This lentiviral vector also contains an EGFP transgene under a separate CMV promoter (see the schematic in Figure 6A). A lentiviral vector containing an efficient hairpin sequence against CD8, an irrelevant gene not expressed in neural progenitors, was used as a control. Both control and DCLK RNAi Lentivirus produced an average of 90%–95% transduction rate in cultured neural progenitor cells (Figure 6).

We first examined the effect of the RNAi Lentivirus on mitotic progression 4 days after transduction. Neural progenitors infected with control Lentivirus were able to progress through M phase, with intact mitotic figures (Figures 6B and 6C). By contrast, 64% of neural progenitors infected with DCLK RNAi Lentivirus were arrested at prometaphase. The integrity of mitotic spindles in the infected neural progenitors was further examined with an α-tubulin antibody. In control cells, stereotypical bipolar spindles formed at metaphase (arrows in Figure 6D). However, in cells infected with DCLK RNAi Lentivirus, the structure of the mitotic spindles was markedly disrupted. The spindles often displayed an asymmetrical morphology with significantly shorter and weaker branches that failed to develop into bipolar spindles (arrowheads in Figure 6D). Consequently, cells were halted at prometaphase and failed to enter metaphase (Figure 6C). Interestingly, we noticed that DCLK RNAi Lentivirus generally seemed to have a less pronounced effect on the microtubule network of interphase cells (asterisks indicates such cells). This may be explained by the possibility that additional MAPs other than DCLK are recruited to stabilize the interphase microtubules, which are much more stable than the spindle microtubules during mitosis (Saxton et al., 1984).

To investigate the impact of the mitotic arrest on cell fate, we first examined whether there was an increase in cell-cycle exit. To this end, BrdU was added to the culture to label S-phase cells after lentiviral infection for 72 hr. 24 hr later, cells were fixed and stained with antibodies against BrdU and Ki67, a proliferation marker for dividing cells in all phases except late G1. Compared to control, cell-cycle-exit index (the percentage of cells that are BrdU positive but Ki67 negative) was significantly increased in cells infected with DCLK RNAi Lentivirus (Figures 6E and 6F; arrows in Figure 6E indicate cells that exited cell cycle). The BrdU labeling index was decreased in neural progenitors infected with DCLK RNAi Lentivirus and the percentage of Ki67 positive cells also decreased, although the difference was not significant (data not shown). This suggests that there might be a reduction in cell proliferation. To examine whether these cells died of apoptosis after they exited the cell cycle, we used a caspase-3 antibody to label apoptotic cells. No significant number of apoptotic cells was detected in either control or DCLK RNAi treatment (data not shown). Abnormal nuclei were not detected in neural progenitors infected with DCLK RNAi Lentivirus; therefore, the neural progenitors appeared to survive the M phase arrest, at least during the experimental time frame. Intriguingly, we detected that a significant percentage of neural progenitors infected with DCLK RNAi Lentivirus became Tuj1 positive (Figures 6G and 6H). These Tuj1-positive cells often developed long and thin processes that resembled axons (arrows in Figure 6G). Note that the percentage of cells that exited the cell cycle (18%) was slightly higher than that of the Tuj1-positive cells (11%), suggesting that a large portion of the cells that prematurely exited the cell cycle terminally differentiated and adopted a neuronal fate.

In Utero DCLK Gain of Function Induces the Differentiation of Neural Progenitors into Cortical Neurons

Next, we directly examined the impact of DCLK gain of function on the fate of cortical neural progenitors in vivo. In utero brain electroporation of DCLK-EGFP or control EGFP was performed at E14 when massive neurogenesis took place in the cerebral cortex. 24 hr later, neural progenitors electroporated with control EGFP were found mostly remained in the SVZ/VZ, whereas about 10% of the electroporated cells migrated to the IZ (arrowheads in Figure 7A). An average of 22.7% of the cells electroporated with control EGFP were labeled with phophoH3, implicating their nature as dividing progenitors (arrows in Figure 7A). By contrast, the majority of neural progenitors electroporated with DCLK-EGFP were detected between IZ and CP, forming a distinguishable ectopic layer (Figures 7A and 7Aa1) (Figure 7Aa1 is the higher power of the boxed region). An average of 4.6% of the neural progenitors overexpressing DCLK were labeled with phosphoH3 (Figures 7A and 7D). By E16, rarely any neural progenitors electroporated with DCLK-EGFP remaining in the SVZ were phophoH3-positive (2 out of 150 cells examined, n = 3) (Figure 7B; arrow in Figure 7Ba2). In addition, many cells further migrated into the CP, displaying a typical morphology of postmitotic migrating neurons (arrowhead in Figure 7Ba3). We further reasoned that if the neural progenitors with DCLK gain of function were committed to a neuronal fate, they might prematurely express layer-specific neuronal markers. To this end, we analyzed the expression of Tbr1, a T-domain transcription factor that is specifically expressed in the glutamatergic cortical neurons produced during early stages of corticogenesis (Englund et al., 2005; Hevner et al., 2001). We found that many cells electroporated with DCLK-EGFP that translocated to IZ became Tbr1 positive. (Arrows in Figure 7Cc2;

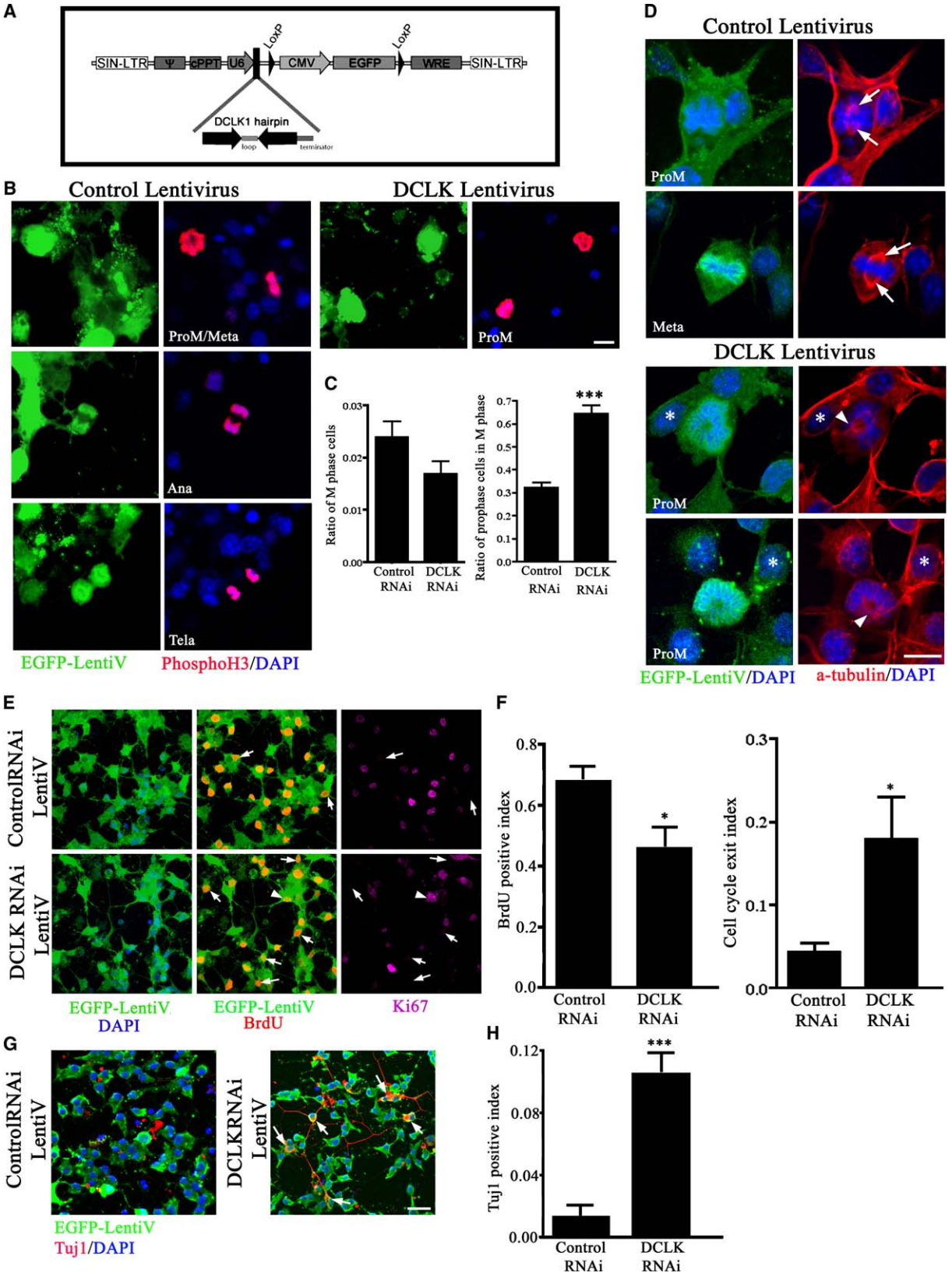

Figure 6. Silencing DCLK by RNAi Lentivirus Disrupts Proper Division of Neural Progenitors and Induces Premature Neuronal Differentiation

(A) Schematic of the lentiviral RNAi construct.

(B and C) Neural progenitors were infected with control or DCLK RNAi Lentivirus. Control RNAi has no effect on mitotic progression. Neural progenitors infected with DCLK RNAi are arrested at prometaphase. Student t test was performed, and triple asterisk indicates $p < 0.001$.

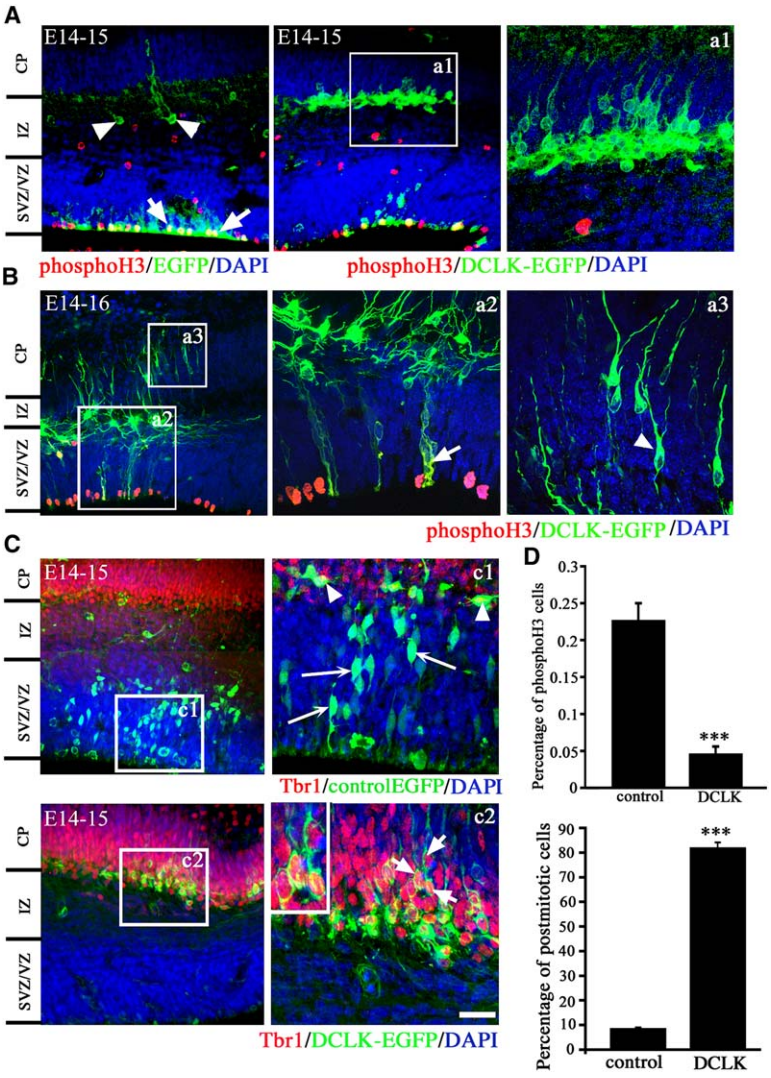

Figure 7. In Utero Electroporation of DCLK Induces Neuronal Identity

In utero electroporation of DCLK-EGFP or control EGFP (green) was performed on E14. (A) By E15, neural progenitors overexpressing EGFP remain mostly in the SVZ/VZ, and many of them express phosphoH3 (indicated by arrows). A few cells exit SVZ/VZ to enter IZ (arrowheads). Cells overexpressing DCLK-EGFP are mostly translocated to the upper IZ and lower CP, and none of them express phosphoH3 (a1). (B) By E16, virtually none of the cells overexpressing DCLK-EGFP are found in M phase (arrow in a2). The majority of them are translocated to the IZ, and many of them further migrate into the CP (arrow in a3). (C) Neural progenitors electroporated with control EGFP remain in the SVZ/VZ and are Tbr1 negative (thin arrows in c1), and only a few cells that reach the border between SVZ and IZ express Tbr1 (arrowheads in c1). Overexpression of DCLK-EGFP induces the translocation of cells from the SVZ to the IZ and the CP. These translocated cells express Tbr1 (arrows in c2, the high power of these cells is also shown in the inset). (D) Quantification of the electroporated neural progenitors that are phosphoH3 positive and those that become postmitotic neurons. Student t tests were performed, and triple asterisk indicates $p < 0.001$. Scale bar in (C) = 100 μm in all panels with lower power and 30 μm in all panels with higher power.

high-power image of these cells is shown in the inset.) By contrast, control neural progenitors that remained largely in the SVZ/VZ were Tbr-1 negative (thin arrows in Figure 7Cc1), with the exception of only a few cells reaching the IZ (arrowheads in Figure 7C; quantification in Figure 7D). These experiments show that overexpression of DCLK in vivo promotes the differentiation of cortical neural progenitors into postmitotic neurons.

In Utero DCLK Loss of Function Alters the Fate of Neural Progenitors

The impact of DCLK loss of function on neural fate in vivo was tested by RNAi lentiviral delivery. On E13, control or DCLK RNAi Lentivirus was introduced into the lateral ventricles to infect neural progenitors lining the ventricular wall. By E16, neural progenitors in the SVZ/VZ infected with control Lentivirus were negative for Tuj1 staining, suggesting that these cells were not postmitotic neurons (thin arrow in Figure 8A). As a result, a distinct Tuj1 boundary can be seen between the proliferating SVZ/VZ and the postmitotic IZ and CP (dotted lines in Figure 8A). In some regions of the SVZ/VZ, cells infected with control Lentivirus migrated toward the IZ, yet still nearly all of them were Tuj1 negative, suggesting a progenitor feature (arrows in Figure 8A). By contrast, many neural progenitors in the SVZ/VZ infected with DCLK RNAi Lentivirus became Tuj1 positive (thin arrows in Figure 8B); thereby, the Tuj1 boundary observed in

(D) In cells infected with control RNAi Lentivirus, mitotic spindle shows a normal bipolar morphology (arrows). In cells infected with DCLK RNAi Lentivirus, the structure of mitotic spindles is disrupted, displays shorter and asymmetrical microtubule branches, and fails to develop into the bipolar structure (arrowheads in [D] indicate such abnormal spindles).

(E and F) Neural progenitors were infected with control or DCLK RNAi Lentivirus and then BrdU and Ki67 were used to analyze the cell-cycle exit index (arrows in [A] point to such cells). There is a decrease of BrdU labeling index and an increase of cell-cycle-exit index after DCLK RNAi treatment. Student t tests were performed, and asterisk indicates $p < 0.01$.

(G and H) Treatment of DCLK RNAi Lentivirus induces a significant neuronal differentiation indicated by Tuj1 staining (arrows in [C] point to differentiated neuronal cells that express Tuj1). Student t tests were performed, and triple asterisk indicates $p < 0.001$. Scale bar in (B) = 10 μm; scale bar in (D) = 10 μm. Scale bar in (E) and (G) = 30 μm.

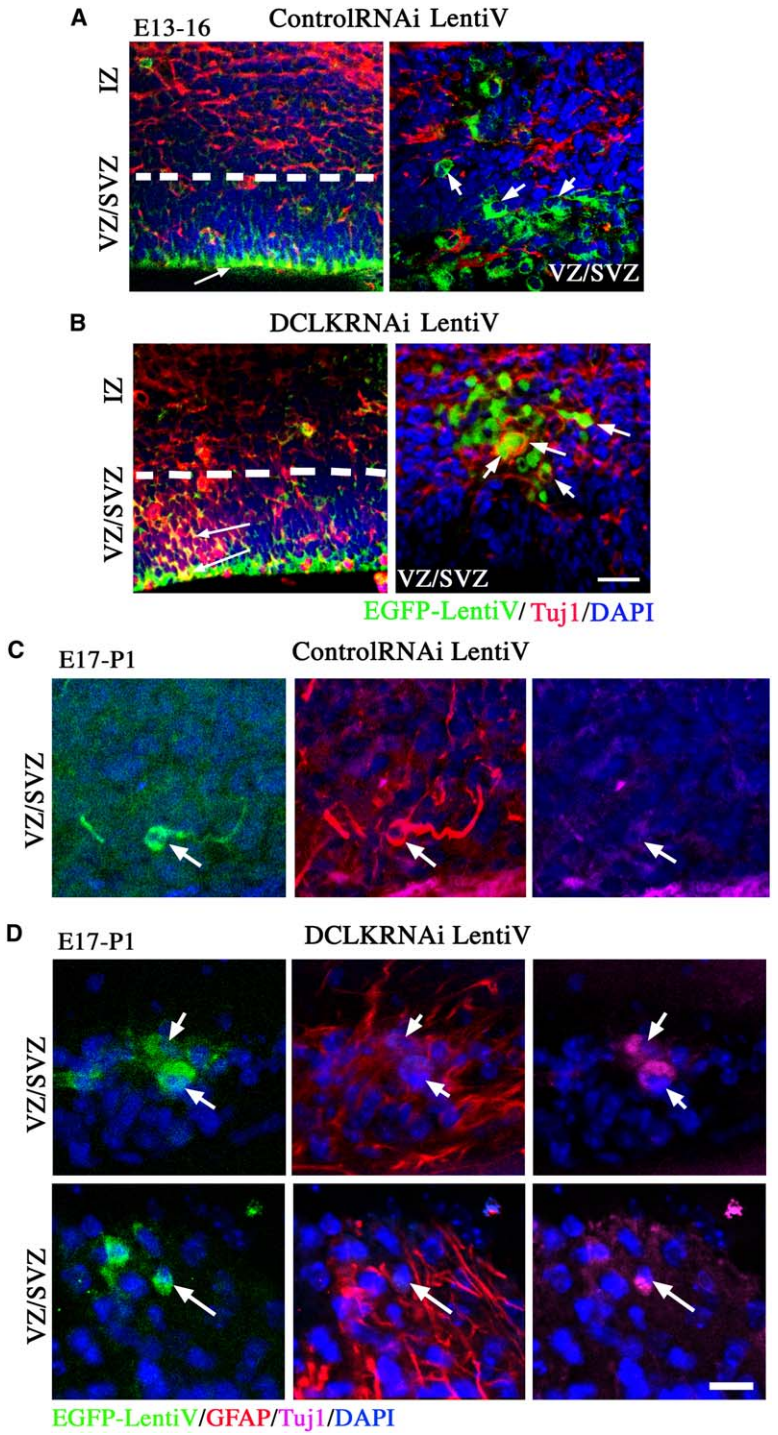

Figure 8. DCLK Loss of Function Promotes Neuronal Differentiation In Vivo

(A and B) Control or DCLK RNAi Lentivirus was delivered into E13 embryonic brain. Neural progenitors infected with control RNAi Lentivirus in the SVZ/VZ are mostly Tuj1 negative (thin arrows in [A] point to infected cells in the SVZ/VZ, and arrows in [A] point to cells in the SVZ migrating toward the intermediate zone). DCLK RNAi induced ectopic neuronal differentiation in the SVZ/VZ (thin arrows in [B] point to such infected cells expressing Tuj1). Some cells in the SVZ migrating toward the intermediate zone also express Tuj1 (arrows in [B]).

(C and D) Control or DCLK RNAi Lentivirus was delivered into the brain on E17, and brains were collected on P1. Cells in the SVZ/VZ infected by control Lentivirus differentiate into glial cells, indicated by the expression of GFAP (arrow in [C]). Cells infected by DCLK RNAi Lentivirus appear to differentiate into Tuj1-positive cells with extremely low expression of GFAP (arrows in [D]) or no expression of GFAP (long arrow in [D]). Scale bar in (B) = 80 μm in panels with lower power in (A) and (B) and 20 μm in panels with higher power in (A) and (B); scale bar in (C) and (D) = 15 μm.

control RNAi infected brains was lost (dotted lines). Many cells en route to the intermediate zone were also frequently found Tuj1 positive (arrows in Figure 8B).

Although in vivo evidence from DCLK gain- and loss-of-function studies appears to advocate the notion that perturbation of DCLK levels favors a neuronal fate, it remains speculative as to whether the primary action of these treatments was to drive progenitors out of the cell cycle. It is possible that once becoming postmitotic, the preference of these cells to adopt a neuronal fate is merely a default response to environmental cues. To determine whether DCLK exerts an instructive role in neuronal fate determination, we delivered DCLK RNAi Lentivirus to E17 brains, and the brains were collected and analyzed on postnatal day (P) 1, a period during which gliogenesis occurs. Compared to E13, less infected cells could be detected at this later time frame. Nonetheless, we found that out of 36 SVZ cells infected by control Lentivirus from three brains randomly selected for confocal microscopy analysis, 32 cells (88.9%) expressed glial fibrillary acidic protein (GFAP), but not discernible Tuj1 (arrow in Figure 8C). In contrast, 29 out of 30 SVZ

cells infected by DCLK Lentivirus displayed robust Tuj1 signal (96.7%) (arrows in Figure 8D). 21 of the 29 Tuj1 positive cells showed very low expression of GFAP, suggesting a probable transition stage from the glial to neuronal fate (arrows in Figure 8D). GFAP signal was not detectable in the remaining 8 Tuj1 positive cells (thin arrow in Figure 8D; Table S1).

To rule out the possibility that defects in neuronal migration contribute to the abnormalities in neurogenesis, we introduced control or DCLK RNAi Lentivirus into E13 embryonic brains and harvested the brains at E19. Surprisingly, no obvious difference in neuronal migration could be detected between control and DCLK RNAi virus infected brains (Figure S4). Likewise, neuronal migration abnormality was not detected in embryonic brains electroporated with DCLK RNAi (Figure S4).

Discussion

Microtubule-associated proteins (MAPs) have long been implicated in various aspects of neural development as well as pathological processes of neurodegeneration (Garcia and Cleveland, 2001; Geschwind, 2003; Tucker, 1990). During development of the CNS, microtubules undergo drastic morphological rearrangements at various stages to achieve tasks such as neuronal division and migration (Tucker, 1990). We found that DCLK regulates the formation of mitotic spindles and the progression of M phase. This, in turn, impacts on the determination of neural fate during neurogenesis.

DCX-Related MAPs with Tandem Microtubule Binding Domains

Classic MAPs, such as MAP1/2 and Tau, are the first identified regulators of microtubules (Al-Bassam et al., 2002; Cassimeris and Spittle, 2001). An expanding pool of "nonclassic" MAPs with microtubule binding domains (MBDs) has recently been shown to stabilize microtubules, possibly through distinct mechanisms (Edelman et al., 2005; Gonczy et al., 2001; Kim et al., 2003; Liu et al., 2004; Sapir et al., 2000; Taylor et al., 2000). This family now includes DCX, DCLK, DCLK2 (with high expression in adult) and RP1 (retinitis pigmentosa 1) in mammals, and ZYG-8 in *C. elegans* (Burgess et al., 1999; Burgess and Reiner, 2000; Edelman et al., 2005; Gleeson et al., 1998, 1999; Gonczy et al., 2001; Liu et al., 2004; Lin et al., 2000). Although both DCX and DCLK are enriched during neural development, DCLK protein is enriched in the active zones of neurogenesis where DCX expression is excluded. This pattern likely warrants a specific role for DCLK during the division of neural progenitors.

The function of DCLK in regulation of the spindle formation is supported by a study in *C. elegans* (Gonczy et al., 2001). ZYG-8, the ortholog of DCLK is required for the positioning and assembly of mitotic spindles during asymmetrical division at one-cell stage. ZYG-8 mutants show disorganized small spindles that highly resemble the phenotype induced by DCLK RNAi in our study. Noticeably, mutations in the kinase domain of ZYG-8 cause a similar defect in spindle formation as those in the MBDs, suggesting that different from DCLK, the kinase domain of Zyg-8 also contributes to the assembly of mitotic spindles (Gonczy et al., 2001). Thus, the function of the kinase domain may be modified through evolution.

It is important to consider that there are many different splice forms of DCLK. There are nine alternative products of the DCLK gene that initiate from two different promoters and display different expression patterns and kinase activities (Burgess and Reiner, 2000, 2002). By using the UCSC Genome Browser, it is possible to identify more than ten additional forms. Interestingly, our RNAi targets the full-length DCLK and potentially smaller variants containing the C-terminal CaMKII homology domain but not the smaller forms containing the N-terminal DCL domain (Figure S5). Therefore, we conclude that DCLK and splice variants containing the C-terminal domain are likely necessary for proper neurogenesis to occur. In this issue of *Neuron*, Koizumi et al. (2005) report that RNAi against exon 2 of DCLK and variants containing the DCL domain causes a marked neuronal positioning abnormality. Taken together, these studies suggest that the distinct domains of DCLK may have different developmental functions.

Potential Mechanism by which DCLK Stabilizes Mitotic Spindles

It was reported recently that DCX preferentially binds to 13 protofilament microtubules and induces their assembly and nucleation (Moores et al., 2004). By using cryo-electron microscopy, DCX was shown wedged in the valley between protofilaments and making contact with four tubulin monomers. The binding of DCX to microtubules is distinct from the classic MAPs such as MAP2 and Tau, which bind the microtubules along the crest of the protofilaments and form an ordered alignment (Al-Bassam et al., 2002; Cassimeris and Spittle, 2001).

Because DCLK and DCX share a high homology at their N terminus, it is likely that DCLK stabilizes microtubules through a similar mechanism. This is further supported by our observation that DCLK and DCL both dramatically stabilize the microtubule spindle structure.

It is well established that dynein plays an essential role during mitosis by functioning as a microtubule-based motor (Rusan et al., 2002; Dujardin and Vallee, 2002). Our data provides evidence that dynein is also required for DCLK to polymerize microtubules. Therefore, it is plausible that dynein facilitates the formation of mitotic spindles in part through distributing DCLK to microtubules. Interestingly, Lis1 was not found to coimmunoprecipitate with DCLK in our study, suggesting that Lis1 indirectly regulates DCLK through dynein.

Regulation of the Formation of Mitotic Spindles

Compared to interphase, the tubulin polymers display a significantly higher turnover rate during M phase, and as a result, the spindle microtubules are 20-fold more dynamic (Saxton et al., 1984). A study with *Xenopus* egg extract showed that microtubule dynamics during mitosis was controlled through the antagonistic activity of the stabilizer XMAP125 and the destabilizer XKCM1 (Tournebize et al., 2000). Interestingly, the in vitro formation of the astral microtubules is largely shortened in egg extract with the depletion of XMAP125, highly resembling the phenotype induced by DCLK RNAi in our study. Conceivably, the regulation of microtubule dynamics in neurons is more intricate. During cortical development,

several microtubule stabilizers such as DCX, LIS1, MAP2, and Tau are abundantly expressed in postmitotic neurons, whereas DCLK seems thus far to be one of the key MAPs expressed in neural progenitors. This expression profile may be a strategy that provides a less robust but sufficient polymerization force during spindle formation, which grants the structure a more dynamic feature.

It is well established that the binding between MAPs and microtubules is regulated by phosphorylation during the cell cycle (Drechsal et al., 1992; Hoehi et al., 1992). For instance, MAP4 and Tau are hyperphosphorylated during mitosis and therefore bind to microtubules with lower affinity (Drechsal et al., 1992; Hoehi et al., 1992). Studies in *Xenopus* showed that cyclin B-cdc2 phosphorylates MAP4, a ubiquitously expressed MAP, at the onset of mitosis upon nuclear envelop breakdown (NEB). This leads to an increment of microtubule turnover that is characteristic of the mitotic spindles (Ookata et al., 1995). More recent studies showed that other important kinases and phosphatases such as CDK5, GSK3β, PKA, MARKs, SADs, and protein phosphatase 2A (PP2A) also play important roles in regulating the binding between MAPs and microtubules (Cruz and Tsai, 2004; Kishi et al., 2005; Schaar et al., 2004; Tanaka et al., 2004b). It is important to test whether some of these kinases and phosphatases present in the neural germinal zone regulate DCLK during mitosis. One potential candidate is MARK4L, an isoform of MARK4, because its expression is restricted to neural progenitors (Beghini et al., 2003).

How Cell Cycle Links to the Cell Fate

Regulation of neural proliferation ultimately controls the size of the brain. Mutations in several genes cause microcephaly (small brain) in humans (Woods, 2004). The affected genes in human microcephaly include Dyrk1 (a mammalian homolog of *Drosophila* minibrain), abnormal spindle in microcephaly (ASPM), microcephalin, and more recently identified CDK5RAP2 and CenPJ (Blagden and Glover, 2003; Bond et al., 2002, 2003, 2005; Fotaki et al., 2002; Hammerle et al., 2002; Jackson et al., 2002). Among these genes, ASPM, microcephalin, CDK5RAP2, and CentPJ have all been found associated with key elements involved in mitosis such as the centrosome and mitotic spindles (Blagden and Glover, 2003; Bond et al., 2002, 2003, 2005; Jackson et al., 2002). By using two-photon time-lapse microscopy to directly visualize mouse cortical neurogenesis, a recent study showed that neural progenitors exhibit two different modes of division, which were proposed to correlate with the neural fate (Haydar et al., 2003). Although this model was challenged by another study showing that asymmetrical distribution of the apical plasma membrane, instead of the division mode, appears to determine the neuronal fate (Kosodo et al., 2004), it is well believed that division mode impacts on the partition of the cell-fate determinants, such as Numb and Catenin (Chenn and Walsh, 2002; Roegiers and Jan, 2004). Curiously, the mitotic spindle rotates rapidly and oscillates consistently within the cells prior to the decision of division mode, suggesting an extremely active selection process for the position on the cell cortex where the plus ends of the astral spindles are to anchor (Haydar et al., 2003; Kaltschmidt et al., 2000). The identity of proteins involved in this process remains unknown although ASPM may be involved in the spindle orientation.

Our results demonstrate a novel element for cell-fate determination, namely, the regulation of cell cycle. A key apparatus that mediates progression of the cell cycle is the mitotic spindle, which is an extremely dynamic structure that demands a fine balance between active microtubule polymerization and depolymerization. Our study suggests that a precise level of DCLK is required to achieve such a balance. Although DCLK gain and loss of function induce opposite morphological alterations of the mitotic spindles, they lead to similar mitotic arrest at prometaphase, suggesting that tilting the balance of spindle morphology in either direction results in aberrant functions that lead to a comparable disruption in the mitotic progression. Interestingly, after arrested cells exit the cell cycle, they appear to adopt, both in vivo and in vitro, a neuronal fate. The mechanism underlying this fate determination is currently unknown; however, it is evident that the observed fate preference is tightly linked to the cell cycle. Without the completion of M phase and the segregation of the two sets of chromosomes, many cellular events essential for fate determination may not occur properly. For example, after neural progenitors are arrested and forced out of the cell cycle at prometaphase, the presence of two additional copies of chromosomes may disrupt chromosomal integrity and lead to genomic instability. As a result, gene transcription that is responsible for either maintaining cells as undifferentiated progenitors or responding to instructive cues to differentiate into glia may be altered. Whether in the long term these cells survive and function as healthy neurons and, furthermore, what causes the adoption of the preferred neuronal fate on the gene regulation level await further investigation.

Experimental Procedures

Purification of MAPs from Neural Tissue

The purification procedure of MAPs from P8 and adult cerebellum follows the standard protocol in Sloboda (1998). All experimental procedures began with the same amount of protein. On average, 30–40 P8 cerebellums and 10–20 adult cerebellums are required and pooled together for each sample. Briefly, tissues were homogenized at a ratio of 1 ml PME buffer per gram brain. After spinning at 150,000 × g for 1 hr, supernatant was recovered and Taxol was added at a final concentration of 20 μM. After incubation at 37ºC for 20 min, the solution was underlain with PME buffer containing 10% sucrose and 10 μM Taxol. The assembled microtubules were collected after spinning at 45,000 × g at 25ºC for 30 min after repeating the procedure once. The MAPs were further isolated from the assembled microtubules with high-concentration salt solution (NaCl, 0.35 M).

Peptide Sample Preparation for Mass Spectrometry

MAPs isolated from P8 and adult cerebellum were resolved by SDS-PAGE. Proteins in the gel were visualized by Coomassie blue staining. Differential protein bands were excised and sliced into 1 mm^3 pieces. A standard in-gel trypsin digestion protocol including carbamidomethylation modification on cystein residues was applied to the sliced gel to yield tryptic peptides. Tryptic digests were extracted by using 10% dimethylformamide in 20 mM ammonium bicarbonate (pH 7.6) and 100% acetonitrile. Extracted peptides were dried and reconstituted in a solution containing 0.1% formic acid and 5% acetonitrile. All peptide samples for mass spectrometry analysis (MALDI-TOF MS, ion trap tandem MS) were desalted by using ZipTipC18 technique. For MALDI-TOF MS, peptides were eluted

from the ZipTips with 10 mg/ml α-cyano-4-hydroxycinnamic acid in 50% acetonitrile, 10% methanol, and spotted on a polished steel target plate.

Mass Spectrometry

MALDI-TOF MS was performed in a Bruker Daltonics's Ultraflex instrument in positive reflecton mode. Laser power was adjusted to 40%–50%. Mass spectra were constructed from 150–300 laser shots, depending on the signal-to-noise ratio. Three-point mass calibration spot was placed next to peptide samples. ProteinProspector (http://prospector.ucsf.edu/) was used for peptide mass fingerprint analysis.

Immunocytochemistry and Western Blot

Immunocytochemistry (ICC) and Western blot (WB) were performed as previously described (Shu et al., 2004). Antibodies used are Nudel (polyclonal; 1:1000 for WB), LIS1 (polyclonal; 1:1000 for WB, 1:50 for ICC), DIC (monoclonal, Santa Cruz, 1:1000 for WB), DHC (polyclonal, Santa Cruz, 1:1000 for WB, 1:100 for ICC), DCX (polyclonal, a gift from Dr. Christopher Walsh, Harvard Medical School, 1:1000 for WB and 1:250 for ICC), DCLK (1:1000 for WB and 1:250 for ICC), βIII-tubulin (monoclonal, Babco, 1:5000 for WB, 1:1000 for ICC), α-tubulin (monoclonal, Sigma, 1:2000 for ICC), phospho H3 (polyclonal, Upstate, 1:200 for ICC), NeuN (monoclonal, Chemicon, 1:1000 for ICC), Ki67 (polyclonal, Novocastra, 1:1000 for ICC), BrdU (monoclonal, Sigma, 1:1000 for ICC), Nestin (monoclonal, BD Bioscience, 1:1000 for ICC), and Tbr-1 (polyclonal, a gift from Dr. Robert F. Hevner, 1:2500 for ICC).

Cell-Cycle Analysis

HEK293 cells were transfected with various plasmids for gain of function or loss of function with lipofectamine (Invitrogen). After 2–3 days, cells were fixed in 4% PFA at room temperature for 10 min followed by 5 min fixation with methanol at −20ºC. The cell cycle was monitored by the morphology of chromosomes stained with both phospho H3, which labels DNA at M phase and DAPI. The mitotic spindles were labeled by α-tubulin antibody. Cells were grouped into different phases of mitosis according to the stereotypical morphology of the DNA and the mitotic spindles.

Coimmunoprecipitation

HEK293 cells were transfected with FLAG-DCLK construct for up to 48 hr. The transfection efficiency was monitored by EGFP expression level. Cells were then lysed in ELB buffer (250 mM NaCl, 0.1% NP-40, 5 mM EDTA, 50 mM Tris [pH 7.5] and proteinase and phosphotase inhibitor cocktail). The cell lysates (0.5–1mg) were incubated with 1 μg anti-FLAG antibody (Sigma) for 1 hr at 4ºC followed by 1 hr of incubation with 40 μl of 50% slurry of protein G Sepharose beads (Amersham Phamacia Biotech). The IPs were run on a gel and processed for Western blotting with antibodies against DIC.

Generation of RNAi Plasmid and Lentivirus

Targeting sequence for DCLK is CCCTTTAAGACTCTGAGAT, which is located at the 3′UTR region of DCLK gene. Oligos for knockdown constructs were purchased from IDT and cloned into the BglII-HindIII sites of pSuper plasmid under H1 promoter.

DHC RNAi and LIS1 RNAi constructs were used as previously reported (Shu et al., 2004). For lentiviral construct, the hairpin sequence was cloned into the HpaI-XhoI sites of pLL3.7 under U6 promoter. An additional nucleotide G was added at the 5′ to facilitate the U6 promoter. Production of VSV-G pseudotped Lentivirus was performed. Briefly, 293FT cells (Invitrogen) were plated into T150 flasks and on the following day, were cotransfected with pLL3.7 transfer and packaging plasmids. The culture media was changed every 24 hr, and the 48 and 72 hr supernatants were collected and pooled. The pooled supernatants were ultracentrifuged in a Beckman SW28 rotor at 25,000 rpm for 1.5 hr and resuspended in 120 μl PBS. Estimates of viral titer were determined by infecting 293FT cells with serial dilutions and assaying GFP expression 48 hr postinfection. Titers ranged from 1–5 × 10^8 infectious units (IFU) per ml.

Neural Progenitor Culture

Mouse neural progenitors were isolated from E14 neocortex and cultured in an 8-well Lab-Trek culture chamber (Nalge Nunc International). The culture medium is made up of Neurobasal medium supplemented with N2 (Gibco) and bFGF-2 at a final concentration of 10 ng/ml (Invitrogen).

In Utero Electroporation and Delivery of Lentivirus

In utero DNA electroporation was performed as previously described (Shu et al., 2004). For the delivery of Lentivirus, E13 embryos were exposed in the uterus, and 1 μl viral particles with a titre of 2 × 10^8 was injected into the lateral ventricle through the uterus wall. On E16, brains were perfused and sectioned on a vibrotome. Brain sections were immunostained with Alexa-488 conjugated anti-EGFP (polyclonal, Molecular Probe, 1:1000) and anti-Tuj1 (monoclonal, Babco, 1:1000).

Supplemental Data

The Supplemental Data for this article can be found online at http://www.neuron.org/cgi/content/full/49/1/25/DC1/.

Acknowledgments

We thank Ms. Xuecai Ge, Mr. Benjamin Samuels, and Dr. Sang Ki Park of Harvard Medical School for technical support and advice on the manuscript. Ms. Michelle Ocana and Mr. Mark Chafel at the Harvard Center for Neurodegeneration and Repair (HCNR) provided us with excellent technical support on the confocal microscopy. We thank Dr. Harold A. Burgess and Dr. Amos Gdalyahu of The Weizmann Institute of Science for DCLK-EGFP and DCLK-FLAG constructs, Dr. Robert F. Hevner of University of Washington for the Tbr1 antibody, and Dr. Christopher A. Walsh of Harvard Medical School and HHMI for the DCX antibody. We are grateful to Joe Gleeson for sharing manuscript prior to publication. T.S. was supported by the Taplin Fellowship and is now funded by Charles A. King Trust Postdoctoral fellowship (Charles A. King Trust, Bank of America Co-Trustee). F.M.C. was supported by the Post-Doctoral Fellowship from the Association pour la Recherche sur le Cancer (Villejuif, France) and currently by the Sir Charles Clore Post-Doctoral Fellowship, (Rehovot, Israel). O.R. is an Incumbent of the Berstein-Mason professorial chair of Neurochemistry. L.-H.T. is a Howard Hughes Medical Institute (HHMI) investigator. This work is partially supported by the National Institutes of Health grant (No. RO3TW007048) and Israeli Science Foundation grant (No.270/04) and support from Nella and Leon Benozyio Center for Neurological Diseases to O.R. and the National Institutes of Health grant (NS37007) to L.-H.T.

Received: May 20, 2005
Revised: August 22, 2005
Accepted: October 19, 2005
Published: January 4, 2006

References

Al-Bassam, J., Ozer, R.S., Safer, D., Halpain, S., and Milligan, R.A. (2002). MAP2 and tau bind longitudinally along the outer ridges of microtubule protofilaments. J. Cell Biol. *157*, 1187–1196.

Baas, P.W. (1999). Microtubules and neuronal polarity: lessons from mitosis. Neuron *22*, 23–31.

Bai, J., Ramos, R.L., Ackman, J.B., Thomas, A.M., Lee, R.V., and LoTurco, J.J. (2003). RNAi reveals doublecortin is required for radial migration in rat neocortex. Nat. Neurosci. *12*, 1277–1283.

Beghini, A., Magnani, I., Roversi, G., Piepoli, T., Di Terlizzi, S., Moroni, R.F., Pollo, B., Fuhrman Conti, A.M., Cowell, J.K., Finocchiaro, G., and Larizza, L. (2003). The neural progenitor-restricted isoform of the MARK4 gene in 19q13.2 is upregulated in human gliomas and overexpressed in a subset of glioblastoma cell lines. Oncogene *22*, 2581–2591.

Blagden, S.P., and Glover, D.M. (2003). Polar expeditions—provisioning the centrosome for mitosis. Nat. Cell Biol. *5*, 505–511.

Bond, J., Roberts, E., Mochida, G.H., Hampshire, D.J., Scott, S., Askham, J.M., Springell, K., Mahadevan, M., Crow, Y.J., Markham, A.F., et al. (2002). ASPM is a major determinant of cerebral cortical size. Nat. Genet. *32*, 316–320.

Bond, J., Scott, S., Hampshire, D.J., Springell, K., Corry, P., Abramowicz, M.J., Mochida, G.H., Hennekam, R.C., Maher, E.R., Fryns, J.P., et al. (2003). Protein truncating mutations in ASPM cause variable reduction in brain size. Am. J. Hum. Genet. *73*, 1170–1177.

Bond, J., Roberts, E., Springell, K., Lizarraga, S., Scott, S., Higgins, J., Hampshire, D.J., Morrison, E.E., Leal, G.F., Silva, E.O., et al. (2005). A centrosomal mechanism involving CDK5RAP2 and CENPJ controls brain size. Nat. Genet. *37*, 353–355.

Burgess, H.A., and Reiner, O. (2000). Doublecortin-like kinase is associated with microtubules in neuronal growth cones. Mol. Cell. Neurosci. *16*, 529–541.

Burgess, H.A., and Reiner, O. (2002). Alternative splice variants of doublecortin-like kinase are differentially expressed and have different kinase activities. J. Biol. Chem. *277*, 17696–17705.

Burgess, H.A., Martinez, S., and Reiner, O. (1999). KIAA0369, doublecortin-like kinase, is expressed during brain development. J. Neurosci. Res. *58*, 567–575.

Cahana, A., Escamez, T., Nowakowski, R.S., Hayes, N.L., Giacobini, M., von Holst, A., Shmueli, O., Sapir, T., McConnell, S.K., Wurst, W., et al. (2001). Targeted mutagenesis of LIS1 disrupts cortical development and LIS1 homodimerization. Proc. Natl. Acad. Sci. USA *98*, 6429–6434.

Cassimeris, L., and Spittle, C. (2001). Regulation of microtubule associated proteins. Int. Rev. Cytol. *210*, 163–226.

Caviness, V.S., Jr., Goto, T., Tarui, T., Takahashi, T., Bhide, P.G., and Nowakowski, R.S. (2003). Cell output, cell cycle duration and neuronal specification: a model of integrated mechanisms of the neocortical proliferative process. Cereb. Cortex *13*, 592–598.

Chenn, A., and Walsh, C.A. (2002). Regulation of cerebral cortical size by control of cell cycle exit in neural precursors. Science *297*, 365–369.

Cruz, J.C., and Tsai, L.H. (2004). A Jekyll and Hyde kinase: roles for Cdk5 in brain development and disease. Curr. Opin. Neurobiol. *14*, 390–394.

Drechsal, D.N., Hyman, A.A., Cobb, M.H., and Kirschner, M.W. (1992). Modulation of dynamic instability of tubulin assembly by the microtubule associated protein tau. Mol Biol Cell. *3*, 1141–1154.

Dujardin, D.L., and Vallee, R.B. (2002). Dynein at the cortex. Curr. Opin. Cell Biol. *14*, 44–49.

Edelman, A.M., Kim, W.Y., Higgins, D., Goldstein, E.G., Oberdoerster, M., and Sigurdson, W. (2005). Doublecortin kinase-2, a novel doublecortin-related protein kinase associated with terminal segments of axons and dendrites. J. Biol. Chem. *280*, 8531–8543.

Englund, C., Fink, A., Lau, C., Pham, D., Daza, R.A., Bulfone, A., Kowalczyk, T., and Hevner, R.F. (2005). Pax6, Tbr2, and Tbr1 are expressed sequentially by radial glia, intermediate progenitor cells, and postmitotic neurons in developing neocortex. J. Neurosci. *25*, 247–251.

Fotaki, V., Dierssen, M., Alcantara, S., Martinez, S., Marti, E., Casas, C., Visa, J., Soriano, E., Estivill, X., and Arbones, M.L. (2002). Dyrk1A haploinsufficiency affects viability and causes developmental delay and abnormal brain morphology in mice. Mol. Cell Biol. *22*, 6636–6647.

Garcia, M.L., and Cleveland, D.W. (2001). Going new places using an old MAP: tau, microtubules and human neurodegenerative disease. Curr. Opin. Cell Biol. *13*, 41–48.

Geschwind, D.H. (2003). Tau phosphorylation, tangles, and neurodegeneration: the chicken or the egg? Neuron *40*, 457–460.

Gleeson, J.G., Allen, K.M., Fox, J.W., Lamperti, E.D., Berkovic, S., Scheffer, I., Cooper, E.C., Dobyns, W.B., Minnerath, S.R., Ross, M.E., and Walsh, C.A. (1998). Doublecortin, a brain-specific gene mutated in human X-linked lissencephaly and double cortex syndrome, encodes a putative signaling protein. Cell *92*, 63–72.

Gleeson, J.G., Lin, P.T., Flanagan, L.A., and Walsh, C.A. (1999). Doublecortin is a microtubule-associated protein and is expressed widely by migrating neurons. Neuron *23*, 257–271.

Goldowitz, D., and Hamre, K. (1998). The cells and molecules that make a cerebellum. Trends Neurosci. *21*, 375–382.

Gonczy, P., Bellanger, J.M., Kirkham, M., Pozniakowski, A., Baumer, K., Phillips, J.B., and Hyman, A.A. (2001). zyg-8, a gene required for spindle positioning in *C. elegans*, encodes a doublecortin-related kinase that promotes microtubule assembly. Dev. Cell *1*, 363–375.

Gupta, A., Tsai, L.H., and Wynshaw-Boris, A. (2002). Life is a journey: a genetic look at neocortical development. Nat. Rev. Genet. *3*, 342–355.

Hammerle, B., Vera-Samper, E., Speicher, S., Arencibia, R., Martinez, S., and Tejedor, F.J. (2002). Mnb/Dyrk1A is transiently expressed and asymmetrically segregated in neural progenitor cells at the transition to neurogenic divisions. Dev. Biol. *246*, 259–273.

Hattori, K., Hattori, M., Adachi, H., Tsujimoto, M., Arai, H., and Inoue, K. (1994). Miller-Dieker lissencephaly gene encodes a subunit of brain platelet-activating factor acetylhydrolase. Nature *370*, 216–218.

Haydar, T.F., Ang, E., Jr., and Rakic, P. (2003). Mitotic spindle rotation and mode of cell division in the developing telencephalon. Proc. Natl. Acad. Sci. USA *100*, 2890–2895.

Hevner, R.F., Shi, L., Justice, N., Hsueh, Y., Sheng, M., Smiga, S., Bulfone, A., Goffinet, A.M., Campagnoni, A.T., and Rubenstein, J.L. (2001). Tbr1 regulates differentiation of the preplate and layer 6. Neuron *29*, 353–366.

Hirotsune, S., Fleck, M.W., Gambello, M.J., Bix, G.J., Chen, A., Clark, G.D., Ledbetter, D.H., McBain, C.J., and Wynshaw-Boris, A. (1998). Graded reduction of Pafah1b1 (LIS1) activity results in neuronal migration defects and early embryonic lethality. Nat. Genet. *19*, 333–339.

Hoehi, M., Ohta, K., Gotoh, Y., Mori, A., Murofushi, H., Sakai, H., and Nishida, E. (1992). Mitogen-activated-protein-kinase-catalyzed phosphorylation of microtubule-associated proteins, microtubule-associated protein 2 and mlcrotubule-associated protein *4*, induces an alteration in their function. Eur. J. Biochem. *203*, 43–52.

Horton, A.C., and Ehlers, M.D. (2003). Neuronal polarity and trafficking. Neuron *40*, 277–295.

Huber, A.B., Kolodkin, A.L., Ginty, D.D., and Cloutier, J.F. (2003). Signaling at the growth cone: ligand-receptor complexes and the control of axon growth and guidance. Annu. Rev. Neurosci. *26*, 509–563.

Jackson, A.P., Eastwood, H., Bell, S.M., Adu, J., Toomes, C., Carr, I.M., Roberts, E., Hampshire, D.J., Crow, Y.J., Mighell, A.J., et al. (2002). Identification of microcephalin, a protein implicated in determining the size of the human brain. Am. J. Hum. Genet. *71*, 136–142.

Kaltschmidt, J.A., Davidson, C.M., Brown, N.H., and Brand, A.H. (2000). Rotation and asymmetry of the mitotic spindle direct asymmetric cell division in the developing central nervous system. Nat. Cell Biol. *2*, 7–12.

Kim, M.H., Cierpicki, T., Derewenda, U., Krowarsch, D., Feng, Y., Devedjiev, Y., Dauter, Z., Walsh, C.A., Otlewski, J., Bushweller, J.H., and Derewenda, Z.S. (2003). The DCX-domain tandems of doublecortin and doublecortin-like kinase. Nat. Struct. Biol. *10*, 324–333.

Kishi, M., Pan, Y.A., Crump, J.G., and Sanes, J.R. (2005). Mammalian SAD kinases are required for neuronal polarization. Science *307*, 929–932.

Koizumi, H., Tanaka, T., and Gleeson, J.G. (2005). *doublecortin-like kinase* functions with *doublecortin* to mediate fiber tract decussation and neuronal migration. Neuron *49*, this issue, 55–66.

Kosodo, Y., Roper, K., Haubensak, W., Marzesco, A.M., Corbeil, D., and Huttner, W.B. (2004). Asymmetric distribution of the apical plasma membrane during neurogenic divisions of mammalian neuroepithelial cells. EMBO J. *23*, 2314–2324.

Lin, P.T., Gleeson, J.G., Corbo, J.C., Flanagan, L., and Walsh, C.A. (2000). DCAMKL1 encodes a protein kinase with homology to doublecortin that regulates microtubule polymerization. J. Neurosci. *20*, 9152–9161.

Liu, Q., Zuo, J., and Pierce, E.A. (2004). The retinitis pigmentosa 1 protein is a photoreceptor microtubule-associated protein. J. Neurosci. *24*, 6427–6436.

Moores, C.A., Perderiset, M., Francis, F., Chelly, J., Houdusse, A., and Milligan, R.A. (2004). Mechanism of microtubule stabilization by doublecortin. Mol. Cell *14*, 833–839.

Ohnuma, S., and Harris, W.A. (2002). Neurogenesis and the cell cycle. Neuron *40*, 199–208.

Ookata, K., Hisanaga, S., Bulinski, J.C., Murofuahi, H., Aizawa, H., Itoh, T.J., Hotani, H., Okumura, E., Tachibana, K., and Kishimoto, T. (1995). Cydln B interaction with microtubule-associated protein 4 (MAP4) targets p34cdc2 kinase to microtubules and is a potential regulator of M-phase microtubule dynamics. J. Cell. Biol. *128*, 849–862.

Paglini, G., Peris, L., Mascotti, F., Quiroga, S., and Caceres, A. (2000). Tau protein function in axonal formation. Neurochem. Res. *25*, 37–42.

Reiner, O., Carrozzo, R., Shen, Y., Wehnert, M., Faustinella, F., Dobyns, W.B., Caskey, C.T., and Ledbetter, D.H. (1993). Isolation of a Miller-Dieker lissencephaly gene containing G protein beta-subunit-like repeats. Nature *364*, 717–721.

Roegiers, F., and Jan, Y.N. (2004). Asymmetric cell division. Curr. Opin. Cell Biol. *16*, 195–205.

Rusan, N.M., Tulu, U.S., Fagerstrom, C., and Wadsworth, P. (2002). Reorganization of the microtubule array in prophase/prometaphase requires cytoplasmic dynein-dependent microtubule transport. J. Cell Biol. *158*, 997–1003.

Sanchez, C., Diaz-Nido, J., and Avila, J. (2000). Phosphorylation of microtubule-associated protein 2 (MAP2) and its relevance for the regulation of the neuronal cytoskeleton function. Prog. Neurobiol. *61*, 133–168.

Sapir, T., Elbaum, M., and Reiner, O. (1997). Reduction of microtubule catastrophe events by LIS1, platelet-activating factor acetylhydrolase subunit. EMBO J. *16*, 6977–6984.

Sapir, T., Horesh, D., Caspi, M., Atlas, R., Burgess, H.A., Wolf, S.G., Francis, F., Chelly, J., Elbaum, M., Pietrokovski, S., and Reiner, O. (2000). Doublecortin mutations cluster in evolutionarily conserved functional domains. Hum. Mol. Genet. *9*, 703–712.

Saxton, W.M., Stemple, D.L., Leslie, R.J., Salmon, E.D., Zavortink, M., and McIntosh, R.J. (1984). Tubulin dynamics in cultured mammalian ceils. J. Cell Biol. *99*, 2175–2186.

Schaar, B.T., Kinoshita, K., and McConnell, S.K. (2004). Doublecortin microtubule affinity is regulated by a balance of kinase and phosphatase activity at the leading edge of migrating neurons. Neuron *41*, 203–213.

Shu, T., Ayala, R., Nguyen, M.D., Xie, Z., Gleeson, J.G., and Tsai, L.H. (2004). Ndel1 operates in a common pathway with LIS1 and cytoplasmic dynein to regulate cortical neuronal positioning. Neuron *44*, 263–277.

Sloboda, R.D. (1998). Isolation of microtubules and MAPs. In Cell: A Laboratory Manuel, D.L. Spector, R.D. Goldman, and L.A. Leinwand, eds. (Cold Spring Harbor, NY: CSHL Press), pp. 54.3–54.22.

Smith, D.S., Niethammer, M., Ayala, R., Zhou, Y., Gambello, M.J., Wynshaw-Boris, A., and Tsai, L.H. (2000). Regulation of cytoplasmic dynein behavior and microtubule organization by mammalian LIS1. Nat. Cell Biol. *2*, 767–775.

Solecki, D.J., Model, L., Gaetz, J., Kapoor, T.M., and Hatten, M.E. (2004). Par6alpha signaling controls glial-guided neuronal migration. Nat. Neurosci. *7*, 1195–1203.

Tanaka, T., Serneo, F.F., Higgins, C., Gambello, M.J., Wynshaw-Boris, A., and Gleeson, J.G. (2004a). LIS1 and doublecortin function with dynein to mediate coupling of the nucleus to the centrosome in neuronal migration. J. Cell Biol. *165*, 709–721.

Tanaka, T., Serneo, F.F., Tseng, H.C., Kulkarni, A.B., Tsai, L.H., and Gleeson, J.G. (2004b). Cdk5 phosphorylation of doublecortin ser297 regulates its effect on neuronal migration. Neuron *41*, 215–227.

Taylor, K.R., Holzer, A.K., Bazan, J.F., Walsh, C.A., and Gleeson, J.G. (2000). Patient mutations in doublecortin define a repeated tubulin-binding domain. J. Biol. Chem. *275*, 34442–34450.

Tessier-Lavigne, M., and Goodman, C.S. (1996). The molecular biology of axon guidance. Science *274*, 1123–1133.

Tournebize, R., Popov, A., Kinoshita, K., Ashford, A.J., Rybina, S., Pozniakovsky, A., Mayer, T.U., Walczak, C.E., Karsenti, E., and Hyman, A.A. (2000). Control of microtubule dynamics by the antagonistic activities of XMAP215 and XKCM1 in *Xenopus* egg extracts. Nat. Cell Biol. *2*, 13–19.

Tucker, R.P. (1990). The roles of microtubule-associated proteins in brain morphogenesis: a review. Brain Res. Brain Res. Rev. *15*, 101–120.

Woods, C.G. (2004). Human microcephaly. Curr. Opin. Neurobiol. *14*, 112–117.

Xie, Z., Sanada, K., Samuels, B.A., Shih, H., and Tsai, L.H. (2003). Serine 732 phosphorylation of FAK by Cdk5 is important for microtubule organization, nuclear movement, and neuronal migration. Cell *114*, 469–482.